한국부식학회지
Journal of the Corrosion Science Society of Korea
Vol. 15, No. 2, June, 1986

Spontaneous Oxidation and Kinetics of Oxide Film Growth of Ti-Code 12#

Young Jin Kim*, Yang Ki Hong**, and R. A. Oriani*

*Corrosion Research Center
University of Minnesota
Minneapolis, Mn 55455
**Department of Mechanical Engineering
Auburn University
Auburn, Alabama 36849

ABSTRACT

The spontaneous oxidation of variously pre-treated Ti-Code 12 specimens in neutral brine solution has been studied by using open-circuit potential measurement. The theoretical values of initial open-circuit potentials calculated by using the mixed potential theory are in good agreement with the experimental data. Furthermore, the changes of potential of Ti-Code 12 specimens at constant anodic current density are measured, and oxide formation rate and reciprocal capacitance data are reported. The high-field approximation is found to be applicable in the present experiment, and parameters for oxide film kinetics are also estimated.

INTRODUCTION

Ti-Code 12 is a primary candidate overpack material for high-level nuclear waste storage in salt beds because of its superior corrosion resistance [1]. Its corrosion properties have been stueied since bedded salt can provide a corrosive environment if water is introduced [2]. Numerous screening tests for corrosion properties of overpack material have shown that Ti-Code 12 is strongly resistant to localized corrosion such as stress corrosion cracking and pitting corrosion, and also to uniform corrosion [3, 4, 5]. However, Ti-Code 12 forms, Ti_2Ni, an intermetallic compound, so that a galvanic corrosion cell might be produced [6]. Also, crevice corrosion was found to be a serious corrosion problem of Ti-Code 12 in brine at 150°C [7].

It is well known that titanium may be embrittled by the presence of small amounts of hydrogen in the metal [8]. A hydride layer is known to form on α-titaniumm during corrosion [9] and subsequent thermal treatment at 200°C and 300°C has been shown to redistribute the hydrogen and cause embrittlement[10]. Hydride formation during exposure to aqueous environ-

#Research supported by the Sandia National Laboratories.

ments may be of significance in understanding of localized corrosion of α-titanium[11] and of titanium alloys in the $\alpha+\beta$ condition, in which hydrides nucleate heterogeneously on dislocations in the α/β interface[12]. Furthermore, if a hydride has formed on the titanium surface, hydrogen absorption rate is observed to be constant[13].

The purpose of this study is to investigate the spontaneous oxidation and galvanostatic anodic oxidation of Ti-Code 12 with respect to behavior of open-circuit potential and kinetics of oxide film growth. The approach has been to study the effect of surface condition of electrode, temperature of electrolyte, anodically applied current density, and amount of hydrogen on spontaneous oxidation and kinetics of oxide film growth of Ti-Code 12 in the brine solution.

EXPERIMENTAL APPROACH

Ti-Code 12, ASTM 12, with the chemical composition given elsewhere[4], used in the present work was supplied by the Sandia National Laboratories. This material was in the form of sheet and discs of 5/8" dismeter and 1/8" thickness were cut from this sheet. Electrical contact to the specimen was accomplished by welding nickel wire to it. The wire was encapsulated in Pyrex-glass tubing and scaled by polyester embedding material. The specimens were polished down to 0.05 μm gamma alumina powder on wet polishing wheels. The specimens were coated with a thin film of microshield lacquer to avoid crevice corrosion between the electrode and the embedding material. The chemical composition of non-deaerated brine solution used as an electrolyte for the measurement of open-circuit potential was shown elsewhere[4]. The pH of this electrolyte, about 6.6, was not adjusted. This solution corresponds to environments likely to be encountered in salt dome and bedded salt situations.

All experiments were done in a cell open to the air, and this cell consisted of a saturated calomel electrode (SCE) as a reference electrode, a working electrode(Ti-Code 12), and a counter electrode(Pt). The reference electrode was isolated from the test solution by means of capillary. The open-circuit potential was measured at 25°C or 80°C as a function of immersion time after variety of pretreatments. These were : (a) air exposure for various times after mechanical polishing (case a), (b) anodic oxidation in 1N H_2SO_4 for various times at +1.2V(SCE) at 25°C (case b), and (c) titanium hydride formation at -1.2 V (SCE) in 1N H_2SO_4 at 25°C for various times (case c). After charging, the specimen was cleaned with deionized water, and was analyzed by X-ray diffraction (Siemens D 500 System) prior to and after open-circuit potential measurement. The potentiostat used for all experiments was a Model 173(Potentiostat/Galvanostat), Model 376(Logarithmic Current Converter), and Model 175(Universal Programmer) from E.G. & G. coupled to a Model 815(X-Y Recorder) from Allen Datagraph Incorporated. Details of process of the hot-vacuum extraction technique for hydrogen analysis were described previously[4].

RESULTS AND DISCUSSION

A. Spontaneous Oxidation

The thickening of the oxide film on Ti-Code 12 was studied by measuring the open-circuit potential. The curves in Figures 1, 2, and 3 represent the variation with immersion time of the open-circuit potential, E_{op}, of Ti-Code 12 in brine at 25°C for previously air-exposed, cathodically charged (titanium hydride formation), and

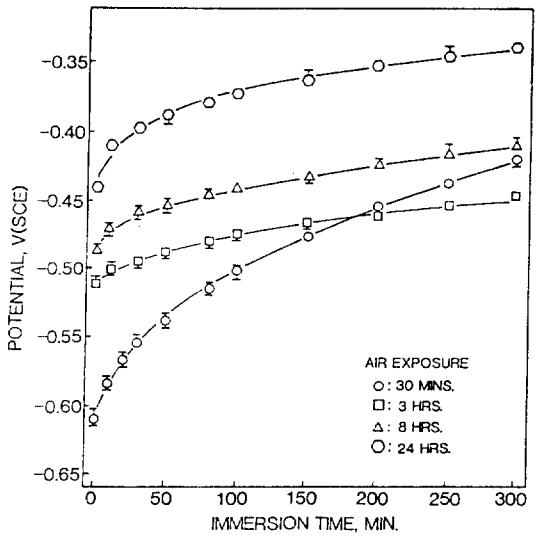

Fig. 1. Effect of prior air exposure on open-circuit potential of Ti-Code 12 in brine at 25℃.

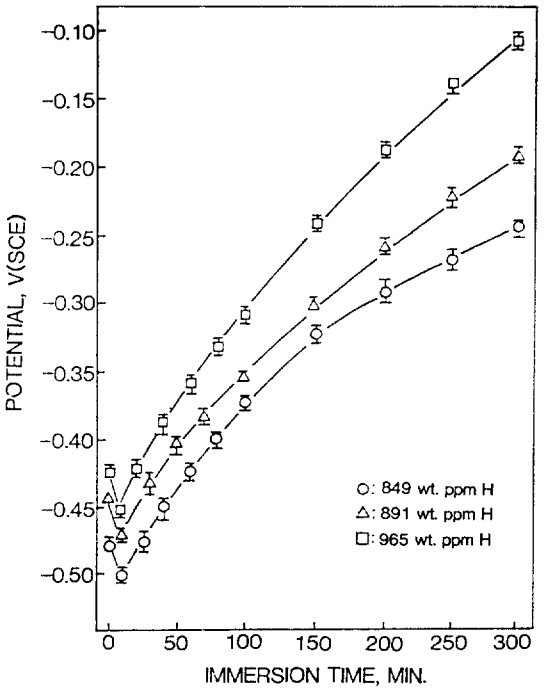

Fig. 2. Effect of cathodic pretreatment on open-circuit potential of Ti-Code 12 in brine at 25℃.

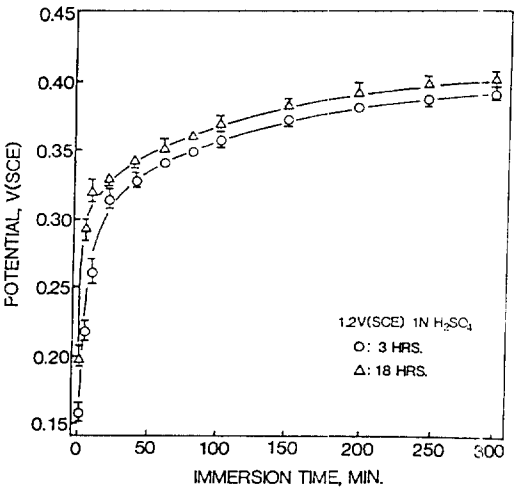

Fig. 3. Effect of anodic pretreatment on open-circuit potential of Ti-Code 12 in brine at 25℃.

anodically oxidized alloy, respectively. The results indicate that the longer is the oxidation or the cathodic charging time, the more noble the potential becomes in either of these cases. The potential at 80°C of the previously air-exposed electrode is more active than that at 25°C (see Figures 1 and 4). In all cases the potential

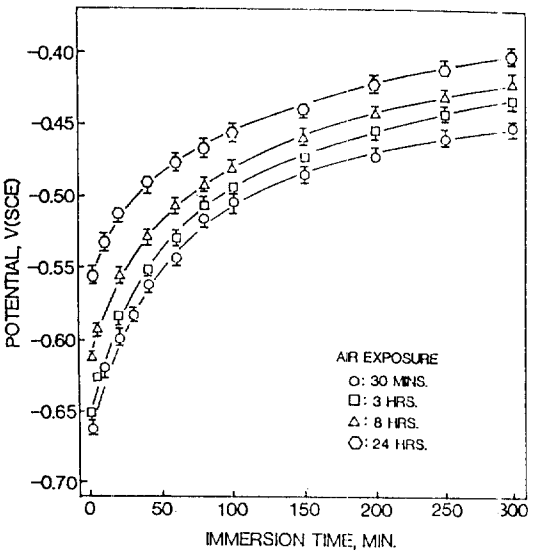

Fig. 4. Effect of prior air exposure on open-circuit potential of Ti-Code 12 in brine at 80℃.

changes in the noble direction with increasing time of immersion. The only exception is the decrease of potential of the cathodically charged electrodes in the first few minutes of immersion. This change in the active direction could be explained by the modified Pourbaix diagram[14] to produce titanium surface which immediately oxidizes. This prediction was confirmed by X-ray diffraction analysis. Figure 5 shows X-ray diffraction lines of hydrided titanium before immersion in brine. Figure 6 shows the new diffraction lines that appear after 300 minutes in brine solution at 25°C. Comparision of Figure 6 with Figure 5 reveals that the new lines, which appeared after free immersion, correspond to titanium lines. The results of X-ray analysis indicate the decomposition of titanium hydride, leaving titanium on the surface of the electrode.

From the experimental values of the initial open-circuit potential and Eh-pH diagram of titanium[15] the initial oxides on the electrodes can be considered to be Ti_2O_3 and Ti_3O_5 for cases (a) and (b), respectively, and these are confirmed by Beck [16] and Tomashov et al [17]. These oxides are subsequently oxidized to TiO_2, which is most stable and protective oxide. For a calculation of the initial open-circuit

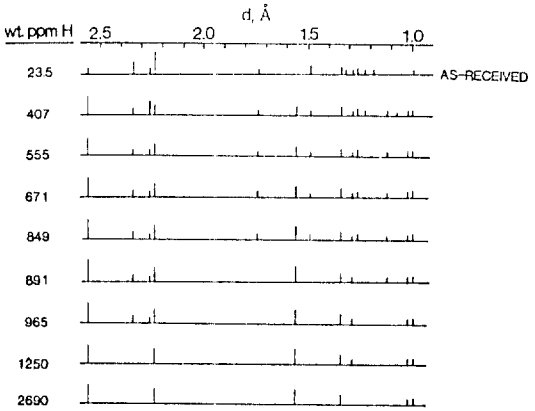

Fig. 5. X-ray diffraction lines after cathodic treatment in 1N H_2SO_4 at 25℃.

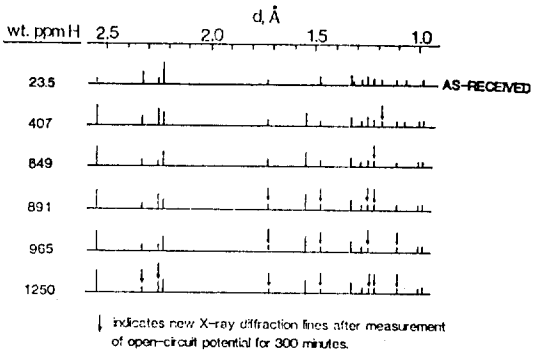

Fig. 6. X-ray diffraction lines after measurement of open-circuit potential for 300 minutes in brine at 25℃, using the cathodically pretreated Ti-Code 12 in 1N H_2SO_4.

potential, the anodic and cathodic reactions are assumed to be:

(i) anodic reaction

case (a): $Ti_2O_3 + H_2O \rightleftharpoons 2TiO_2(hydr) + 2H^+ + 2e$ (1)

case (b): $Ti_3O_5 + H_2O \rightleftharpoons 3TiO_2(hydr) + 2H^+ + 2e$ (2)

case (c): $TiH_2 \rightleftharpoons Ti + 2H^+ + 2e$ (3)

(ii) cathodic reaction

$$4OH^- \rightleftharpoons O_2 + 2H_2O + 4e \quad (4)$$

Under the condition of the present experiments, the reduction of O_2 represents the most significant cathodic reaction.

For a case of anodically pre-oxidized electrode (case b), one can consider the following two reactions:

(i) anodic reaction

$$Ti_3O_5 + H_2O \underset{k_2}{\overset{k_1}{\rightleftharpoons}} 3TiO_2(hydr) + 2H^+ + 2e \quad (2)$$

(ii) cathodic reaction

$$4OH^- \underset{k_4}{\overset{k_3}{\rightleftharpoons}} O_2 + 2H_2O + 4e \qquad (4)$$

where k_1, k_2, k_3, and k_4 are the specific rate constants. The initial open-circuit potential can be calculated as a mixed potential by using the Butler-Volmer equation for each partial reaction,

$$i_a = 2k_1 e^{\alpha FE/RT} - 2k_2 [H^+]^2 e^{-(1-\alpha)FE/RT} \qquad (5)$$

$$i_c = 4k_3 [OH^-]^4 e^{\beta FE/RT} - 4k_4 [O_2] e^{-(1-\beta)FE/RT} \qquad (6)$$

where α, β = charge transfer coefficients. At the mixed potential E_m, $i_a = -i_c$, and assuming $\alpha = \beta = 0.5$, the equations (5) and (6) can be solved to give

$$\exp\left(\frac{-FE_m}{RT}\right) = \left(\frac{k_1 - 2k_3 [OH^-]^4}{2k_4 - k_2 [H^+]^2}\right) \qquad (7)$$

The equation (7) can be greatly simplified if the back reaction is considered negligible. This seems to be a reasonable assumption since we find experimentally that the rate of increase of the open-circuit potential is large, which indicates that a large overvoltage exists. Then the expression becomes

$$\exp\left(\frac{-FE_m}{RT}\right) = \left(\frac{k_1}{2k_4}\right) \qquad (8)$$

The overall reaction for equation (8) is

$$2Ti_3O_5 + O_2 + 4H_2O \underset{k_4}{\overset{k_1}{\rightleftharpoons}} 6TiO_2(hydr) + 4H^+ + 4OH^- \qquad (9)$$

Hence, one can rewrite equation (8)

$$\exp\left(\frac{-FE_m}{RT}\right) = \frac{K}{2} \qquad (10)$$

where K = equilibrium constant of the overall reaction. Substituting thermodynamic data[15] into equation (10) to obtain the value of K for the overall reaction, then the initial open-circuit potential can be calculated at 25°C as

$$E_{m,b} = -0.03 \text{ V(SCE)}$$

Using the same method as above, the initial open-circuit potentials of cases (a) and (b) are, respectively

$$E_{m,a} = -1.27 \text{ V(SCE)}$$

$$E_{m,c} = +0.34 \text{ V(SCE)}$$

The theoretically calculated and experimental initial open-circuit potentials are shown in Figure 7 for three cases. The theoretically calculated

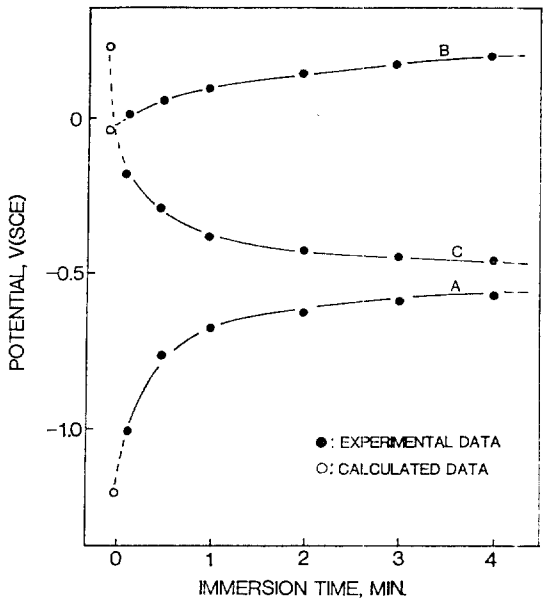

Fig. 7. Plot of open-circuit potentials vs. immersion time with the calculated and measured potentials. (A) air-exposed Ti-Code 12. (B) anodically oxidized Ti-Code 12. (C) cathodically charged Ti-Code 12.

initial potentials are more active than the experimental values for the air-exposed and the anodically oxidized electrodes, but the calculated value for the cathodically charged electrode is more noble than the experimental potential. These disparities can be understood by recognizing that the initial rate of change of the open-circuit potential is too rapid for the measuring speed of the apparatus employed. In each of three cases, the potential changes with immersion time in the noble direction, and this is characteristic of spontaneous passivation as a result of oxide film formation. This rate is high at the beginning of immersion, and decreases with time but does not reach a constant value within the duration of the experiment. In case (c), titanium hydride decomposition is followed by the oxide formation. The open-circuit potentials in all cases lie in the passive potential region as shown in Figure 8, which indicates the protective oxide formation.

B. Galvanostatic Film Formation

Ti-Code 12 electrode conditioned according to one of the previously described pretreatments was maintained in the brine solution at a constant applied anodic current density in the range of 0.05 $\mu A/cm^2$ to 1.0 $\mu A/cm^2$. The change of potential with time was recorded from 1 to 300 minutes after immersion.

The resulting curve was very sensitive to the kind of treatment of the electrode. The results obtained with prior air-exposed, anodically oxidized, and cathodically charged electrodes are shown in Figures 9, 10, and 11, respectively. The potential curves show well defined linear regions before deviating from linearity at later times of polarization in the cases of air-exposed and potentiostatically oxidized electrodes. The slopes of the E - t curves in the linear region increase with increase of applied anodic current density. The cathodically charged electrodes show a decrease in potential followed by a linear

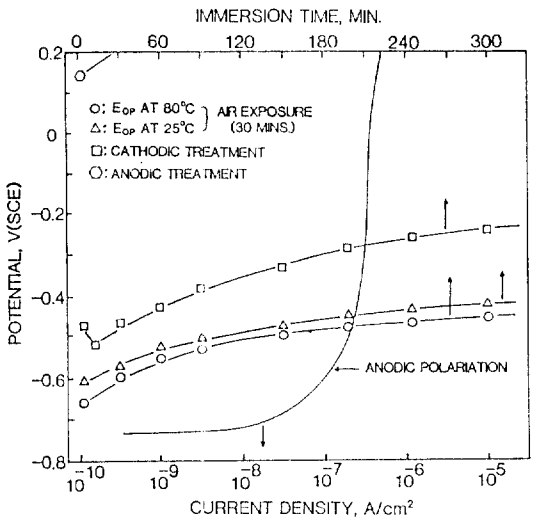

Fig. 8. Plot of open-circuit potentials and anodic polarization curve of Ti-Code 12 in brine at 25℃.

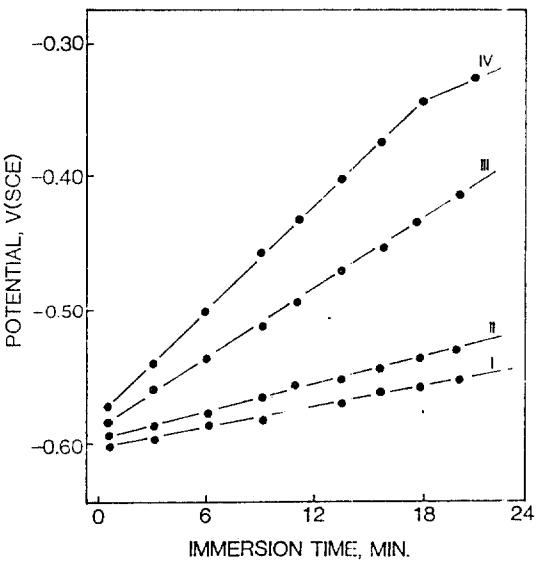

Fig. 9. Potential-time curves in brine at 25℃, of Ti-Code 12 previously air-exposed for 30 minutes. Galvanostatic anodic current densities: (I) 0.05 $\mu A/cm^2$. (II) 0.1 $\mu A/cm^2$. (III) 0.4 $\mu A/cm^2$. (IV) 0.7 $\mu A/cm^2$.

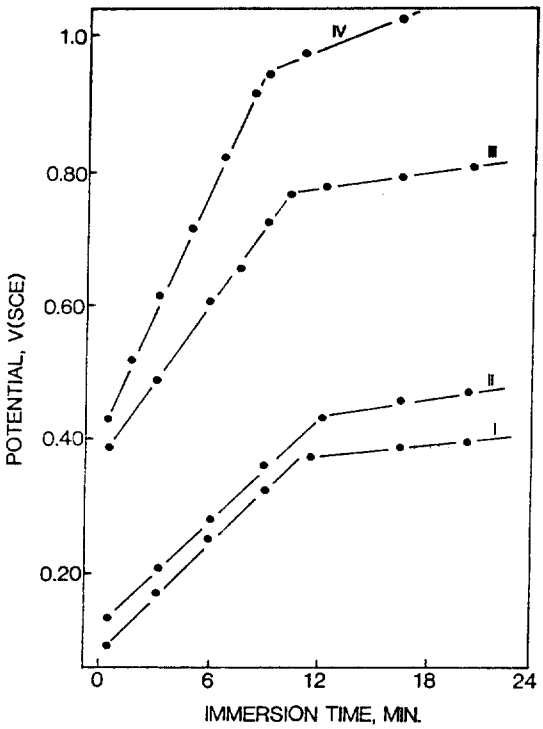

Fig. 10. Potential-time curves in brine at 25℃, of Ti-Code 12 previously anodically oxidized for 3 hours in 1N H_2SO_4.
Galvanostatic anodic current densities: (I) 0.05μA/cm². (II) 0.07μA/cm². (III) 0.1μA/cm². (IV) 0.4μA/cm².

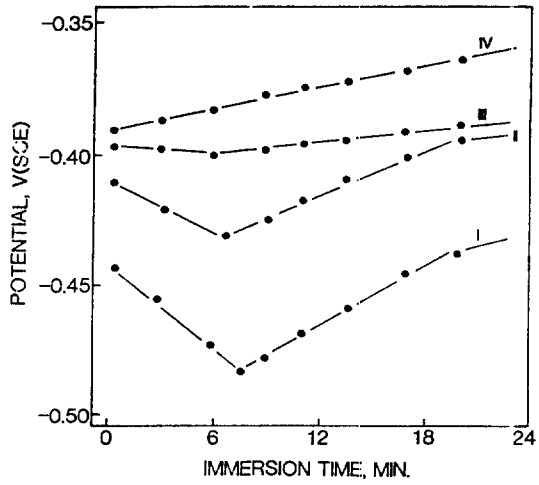

Fig. 11. Potential-time curves in brine at 25℃, of Ti-Code 12 cathodically pre-treated to produce 849 wt. ppm H. Galvanostatic current densities: (I) 0.05μA/cm². (II) 0.1μA/cm². (III) 0.5μA/cm². (IV) 1.0μA/cm².

increase. The decrease at beginning of polarization may be explained as a result of the occurence of more than one anodic process, e.g. anodic decomposition of titanium hydride and anodic film formation. The decomposition of titanium hydride predominates at the beginning of polarization, thus leading to bare metal. Passive oxide film then forms and this is accompanied by the rise of potential. Duration of the period when decomposition of titanium hydride predominates decreases with increasing anodic current density, as shown in Figure 11.

Film formation by direct interaction between metal and solution (H_2O, OH^-, and other anions) is often the case. Anodic dissolution and film growth may occur simultaneously, although with different rates. If the rate of dissolution is much high than that of film growth, corrosion continues and the potential decreases. It has been shown that no decreasing potential with immersion time was observed so that the film grows at certain oxide film growth rate. Thus, polarization leads to film thickening by means of ion conduction. As shown in Figures 9 and 10, the slope of E vs. t increases with increasing current, which indicates the efficiency for oxide growth on Ti-Code 12 with increase of anodic current density. Therefore, anodic dissolution can be neglected in the present study. The increase of oxide film thickness with time at constant anodic current density results in a corresponding increase of potential in order to maintain a constant electric field strength. Hence, potential increases linearly with time toward noble direction.

(i) Oxide Film Thickness

The increase of oxide film thickness, $\Delta\delta$,

over the time interval, Δt, can be calculated from $\Delta\delta = (M\, i_a \Delta t) / (nF\rho\sigma)$, where σ is the roughness factor, M is the molecular weight of oxide, ρ is its density, i_a is the anodic current density, nF is is the number of coulombs required for the formation of one mole of oxide. For constant anodic current density one can write:

$$dQ = i_a\, dt = \left(\frac{nF\rho\sigma}{M}\right) d\delta \qquad (11)$$

where dQ is the quantity of electricity. From equation (11), one can get,

$$\left(\frac{d\delta}{dt}\right) = \left(\frac{M\, i_a}{nF\rho\sigma}\right) \qquad (12)$$

provided that the only anodic reaction is that for the formation of oxide film, otherwise

$$\left(\frac{d\delta}{dt}\right) = \left(\frac{M}{nF\rho\sigma}\right)(i_a - i_d)$$

where i_d represents the electronic current for anodic dissolution of oxide.

Before immersion of the electrode, a pre-formed oxide layer of thickness δ_o was obtained. This initial thickness depends on the previous treatment of electrode, as described in a previous section. During galvanostatic oxidation film growth may occur by the transport of positive ions through the oxide to the oxide/solution interface, or by transport of oxide ions in the opposite direction. Integration of Eq. (12) gives the oxide thickness at a given immersion time as

$$\int_{\delta_o}^{\delta} d\delta = \left(\frac{M\, i_a}{nF\rho\sigma}\right) \int_o^t dt$$

$$\delta = \delta_o + \left(\frac{M\, i_a}{nF\rho\sigma}\right) t \qquad (13)$$

In order to estimate the pre-formed oxide thickness, one can get the following equation with field strength H,[18]

$$i_a = A \exp(BH) = A \exp\left[\frac{BE_f}{\delta_o + \left(\frac{Mi_a}{nF\rho\sigma}\right) t}\right] \qquad (14)$$

where A and B are constants and E_f the potential drop across the oxide layer. Taking logarithm of both sides of Eq. (14), one can rewrite

$$\log i_a = \log A + \left(\frac{1}{2.303}\right)\left[\frac{BE_f}{\delta_o + \left(\frac{Mi_a}{nF\rho\sigma}\right) t}\right]$$

$$E_f = \frac{2.303}{B}\left[\delta_o + \left(\frac{Mi_a}{nF\rho\sigma}\right) t\right] \log\left(\frac{i_a}{A}\right)$$

$$\left(\frac{dE_f}{d \log i_a}\right)_Q = \left(\frac{2.303}{B}\right)\left[\delta_o + \left(\frac{MQ}{nF\rho\sigma}\right)\right] \qquad (15)$$

From the slope of straight line of E vs. $\log i_a$ as shown in Figure 12, pre-formed oxide thickness can be estimated.

(ii) Parameters of Oxide Growth

Oxides of titanium are poor electron conductor, and charge transfer is predominantly ionic[19]. During the oxide film growth the ionic current density is an exponential function of the field strength, H,

$$i_a = A \exp(BH) \qquad (14)$$

The total potential difference between the electrode and a suitable reference electrode consits of the potential difference across the oxide film E_f, and the sum of interfacial potentials, ϕ, at metal/

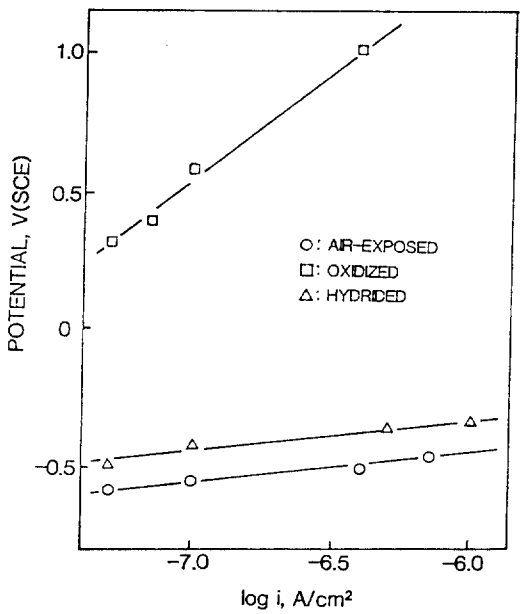

Fig. 12. Potential/log i relations at constant Q (t=8 minutes).

oxide and oxide/solution boundaries. Thus one can write

$$E = E_f + \phi = E_f + \text{constant} \qquad (16)$$

Therefore, the observed increase of potential is the increase of potential across the oxide layer. From Eq. (14),

$$\ln\left(\frac{i_a}{A}\right) = \left[\frac{BE_f}{\delta_o + \left(\frac{Mi_a}{nF\rho\sigma}\right)t}\right] \qquad (17)$$

Rearrangement of the above equation gives

$$E_f = \left(\frac{\delta_o}{B}\right) + \left(\frac{Mi_a\, t}{BnF\rho\sigma}\right) \ln\left(\frac{i_a}{A}\right) \qquad (18)$$

After replacing E for E_f one can get

$$E - \phi = \left(\frac{\delta_o}{B}\right) + \left(\frac{Mi_a t}{BnF\rho\sigma}\right) \ln\left(\frac{i_a}{A}\right)$$

$$E = \phi + \left(\frac{\delta_o}{B}\right) + \left(\frac{Mi_a\, t}{BnF\rho\sigma}\right) \ln\left(\frac{i_a}{A}\right) \qquad (19)$$

where E is the measured potential. Differentiating the Eq. (19) with respect to time t at constant i_a,

$$\left(\frac{dE}{dt}\right)_{i_a} = \left(\frac{Mi_a}{BnF\rho\sigma}\right) \ln\left(\frac{i_a}{A}\right) \qquad (20)$$

When the oxide film thickness increases with time at constant i, E_f and consequently E must be increased to keep the current density constant. Equation (20) represents the oxide film formation rate. Therefore, the experimental linear relation between E and t is evidence for the validity of the high-field approximation. The linear potential rise, as shown in Figures 9, 10, and 11, indicates the validity of Eq. (20).

Dividing both sides of Eq. (20) by the current density, one can get

$$\left(\frac{i}{i_a}\right)\left(\frac{dE}{dt}\right)_{i_a} = 2.303\left(\frac{M}{BnF\rho\sigma}\right) \log\left(\frac{i_a}{A}\right) \qquad (21)$$

Also, one can get

$$\left(\frac{i}{i_a}\right)\left(\frac{dE}{dt}\right)_{i_a} = \left(\frac{1}{C}\right)$$

where C is a pseudo-capacitance. Thus, a plot of reciprocal pseudo-capacitance vs. log i_a should give a straight line; this is shown in Figure 13 for the previously air-exposed and previously anodically oxidized electrodes. The slopes and intersects of these straight lines were used for the calculation of A and (σB). For TiO_2, M = 79.9 g/mole and d = 3.84 g/cm^2, and $M/nF\rho$ = 5.4x 10^{-5} cm^3/coulomb. Using these values, A and σB for the air-exposed and anodically oxidized electrodes are given in Table 1. The value of A is the

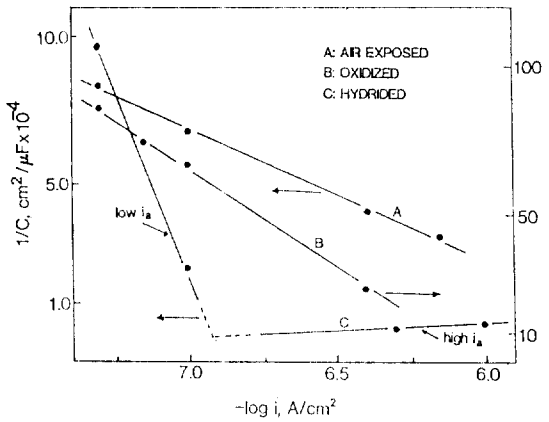

Fig. 13. Relation between reciprocal capacitance and log i in brine at 25℃

Table 1. Parameters of oxide film growth in brine.

ELECTRODE	A (A/cm^2)	σB (cm/V)
AIR EXPOSURE	4.9×10^{-8}	2.76×10^{-5}
ANODIC OXIDATION	4.9×10^{-8}	1.86×10^{-6}

same for the two pretreatments of the electrodes, while σB of the anodically oxidized electrode is smaller than that of the air-exposed one. Since the oxide film thickness is proportional to pseudo-capacitance i.e.,

$$\Delta\delta = \left(\frac{M\,\Delta Q}{nF\rho\sigma}\right) = \left(\frac{MC\Delta E}{nF\rho\sigma}\right)$$

the larger 1/C is, the thinner is the oxide film formed. Therefore, the oxide film formed after polarization on the previously air-exposed electrode is thicker than that on the previously anodically oxidized one. This difference is attributable to the thicker pre-formed film on the previously oxidized electrode.

In the case of the cathodically charged electrode, the duration of decomposition of titanium hydride lasted longer at lower applied current densities than at higher current densities, but the trend is reversed at longer time as shown in Figure 11. This change of slope produces the breaking point on the plot of (1/C) vs. log i in Figure 13. However, oxide formation on the titanium hydride and titanium occurs simultaneously. But explanations of the breaking point for the cathodically charged electrode on the plot of (1/C) vs. log i still remain open.

(iii) Electric Field Strength

From Eqs. (14) and (21), one can obtain

$$BH = 2.303 \log (i_a/A)$$

and it follows that

$$H/\sigma = (nF\rho / MC) \qquad (22)$$

H/σ thus can be calculated from the reciprocal pseudo-capacitance data at constant current density shown in Figure 13. The results, given in Table 2 for the case of the previously air-exposed and anodically oxidized electrodes, indicate that (i) the value of H/σ for the anodically oxidized electrode is lower than that for the air-exposed one, and (ii) the increase in the current density increases H/σ for both cases. From the value B, the effective activation distance $a^* = kTB/q$, where q is the charge on the ion, can be calculated. This is related to the barrier width. Because

Table 2. Electric field strength.

AIR EXPOSURE		ANODIC OXIDATION	
i_a ($\mu A/cm^2$)	H/σ (V/cm)	i_a ($\mu A/cm^2$)	H/σ (V/cm)
0.05	2.18×10^7	0.05	2.15×10^6
0.1	2.81×10^7	0.07	2.49×10^6
0.4	4.47×10^7	0.1	3.05×10^6
0.7	5.45×10^7	0.4	7.41×10^6

of uncertainty in the roughness factor σ, a* values are not reported in the present study.

The experimental data for oxide film formation by galvanostatic oxidation are consistent with the high-field approximation. This is true for cases a and b pretreatments of the electrodes. The kinetic parameters for oxide growth A, B, and H are obtained. The shape of potential/time curve at constant current density depends on the pretreatment of electrode.

CONCLUSION

From the present studies, the following conclusions can be reached:

(A) Spontaneous Oxidation

(1) Spontaneous oxidation is accompanied by thickening for prior air-exposed and prior anodically oxidized Ti-Code 12. Decomposition of titanium hydride on previously cathodically charged Ti-Code 12 occurs initially and is followed by oxide film thickening.

(2) Oxide thickening rate is fast initially and slow later.

(3) Open-circuit potentials of previously anodically oxidized Ti-Code 12 are more noble than those of previously cathodically charged and prior air-exposed electrodes during the oxide growth.

(4) The initial open-circuit potentials calculated by using the mixed potential theory are in good agreement with experimental values.

(5) The high-field approximation applies to the present studies of spontaneous oxidation.

(B). Galvanostatic Film Formation

(1) The oxide film growth follows the high-field ionic conduction mechanism.

(2) The high-field approximation, $i = A \exp(BH)$, is valid. This is supported by the linearity obtained between the reciprocal pseudo-capacitance vs. log i and the potential vs. log i at constant charge.

(3) Data are given for the kinetics parameters and for those for electric field strength.

ACKNOWLEDGEMENT

This work was supported by the Sandia National Laboratories, a Department of Energy Facility, under Sandia Contract 68-0273.

REFERENCES

1. L. Abrego and H. J. Rack, Presented at NACE, Corrosion/81, Toronto, Canada, April 6-10, 1981.
2. J. W. Braithwaite and M. A. Molecke, Nuclear and Chemical Management, 1, 37 (1980).
3. M. A. Molecke, D. W. Schaefer, R. S. Glass, and J. A. Ruppen, Sandia Report, SAND 81-1585, 1981.
4. Y. J. Kim, Y. K. Hong, R. A. Oriani, and H. S. Isbin, *Proc. of Sym. on Waste Management '84*, V-1, p 619, edited by R. G. Post, 1984.
5. Y. J. Kim and R. A. Oriani, Submitted for publication to Corrosion.
6. R. S. Glass, Electrochimica Acta, 28, 1507 (1983).
7. T. M. Ahn, H. Jain, and P. Soo, Presented at ECS meeting, Detroit, 1982.

8. R. I Jaffe and N. E. Promisel, *The Sci. Tech. and Appl. of Titanium*, Pergamon Press, Oxford (1970).
9. E. L. Owen et al., Corrosion, **28**, 292 (1972)
10. I. I. Phillips, P. Poole, and L. L. Shreir, Corr. Sci., **12**, 855 (1972).
11. D. T. Powell and J. C. Scully, Corr. Sci., **10**, 719(1970).
12. G. F. Pittnato and W. D. Hanna, Metall. Trans., **3**, November (1972).
13. R. D. Wasilewski and G. L. Kehl, Metallurgica, **XI(50)**, 301(1954).
14. M. J. Blackburn, J. A. Feeney, and T. R. Beck, in "*Advances in Corr. Sci. and Tech.*" M. G. Fontana and R. W. Staehle, eds., V-3, p. 67-292, Plenum Press, N.Y. (1973)
15. M. Pourbaix, *Atlas of Electrochemical Equilibria*, NACE, Houston, 1974.
16. T. R. Beck, *Passivity of Metals*, edited by R. P. Frankendal and J. Kruger, ECS Inc., Princeton, New Jersey, 1978.
17. N. D. Tomashov and P. M. Al'tovskii, *Corrosion and Protection of Ti*, Government Scientific-Technical Publication of Machine-Building Literature, Moscow, 1963.
18. A. Guntherschulze and H. Betz, Z. Phys., **91**, 70(1934), **92**, 367(1934).
19. C. D. Hall and N. Hackerman, J. Phy. Chem., **57**, 262(1953).